Structurally induced large changes of the energy level alignment in CuPc on Cu(110)-(2 × 1)O

Bret Maughan,[1] Calley N. Eads,[1] Percy Zahl,[2] and Oliver L. A. Monti[1,3,*]

[1]*University of Arizona, Department of Chemistry & Biochemistry, 1306 E. University Blvd., Tucson, Arizona 85721, USA*

[2]*Brookhaven National Laboratory, Center for Functional Nanomaterials, Upton, New York 11973, USA*

[3]*University of Arizona, Department of Physics, 1118 E. Fourth Street, Tucson, Arizona 85721, USA*

(Received 4 April 2018; revised manuscript received 10 September 2018; published 2 October 2018)

While it is becoming apparent that organic semiconductor/metal interfaces may exhibit a variety of different structural phases, it is at present unclear to what extent these different thin-film structures determine the interfacial electronic structure. Here, we observe large changes in the interfacial electronic structure for the case of copper(II) phthalocyanine (CuPc) on Cu(110)-(2 × 1)O. This striking evolution of the interfacial electronic structure occurs beyond the first monolayer of CuPc and is particularly evident in the frontier orbital region. Using scanning tunneling microscopy in conjunction with photoemission spectroscopy, we characterize ultrathin films of CuPc grown on oxygen reconstructed Cu(110). We propose that the observed unique changes to the electronic structure result from an abrupt transition in film structure between the first and second layers: An interface layer of ordered, face-on molecules templates a largely vertical, edge-on orientation of molecules in the subsequent layer. The quadrupole moment of the molecule accounts for the sizable and unusual change in ionization energy between molecules in the two layers. Our results demonstrate that the precise structure of the organic semiconductor film exerts an important role in determining the interfacial electronic structure that must be considered and may be harnessed for tailoring energy level alignment at such interfaces.

DOI: 10.1103/PhysRevB.98.155106

I. INTRODUCTION

A central motivation for studying organic semiconductors and their interfaces is the desire to discover new materials and materials combinations that improve on functionality, power, and efficiency of modern electronic devices [1–3]. The field has advanced rapidly in recent years and, as a result, molecular-based devices are starting to be competitive with traditional semiconductor devices in commercial optoelectronic applications such as, e.g., photovoltaic and visual display technologies [4]. Organic semiconductors also hold additional value as promising components in next-generation device applications where shrinking device scale, biocompatibility, and mechanical flexibility are primary objectives.

Central to efforts for tailoring device properties has been the recognition that the interfaces between the organic semiconductor and, e.g., the metal contacts may determine to a large measure overall device function and efficiency. As the result of advances made both in experiment and theory, there are by now a range of models that offer a certain level of explanatory power of the electronic structure of specific types of interfaces [5–10]. Molecular self-assembly and the structure of the organic semiconductor film is implicitly and sometimes explicitly a key ingredient in all of these models. This is important, since organic thin films may exhibit a plethora of different phases and structures over often a small temperature and coverage range, and one may expect as a result different interfacial electronic structures associated with each thin-film phase [11–13]. The scientific challenge derives then from a need to understand *how* these different thin-film structures influence the interfacial electronic structure, and in turn to what extent thin-film structure may be ultimately tailored to enhance desirable device properties. Clearly, a combination of methods that provide structure and energy levels is necessary to achieve this goal.

Some insight into this question may be gained from varying the nature of the organic semiconductor [14], the substrate crystal face on which the film is grown [15], or from introducing interlayers [16,17]. These methods draw strength from the rich diversity of available molecular platforms and the specific interactions with distinct surfaces, but require a comparison across inherently different interfaces. In contrast, structural transitions and associated control of the interfacial electronic structure for a single organic/metal interface are much rarer [11–13,18], but offer an important and internally consistent step toward a deeper understanding of the forces that control interfacial electronic structure and energy-level alignment. This has the advantage of observing molecular-level structural changes while preserving both the bulk metallic electronic structure and the chemical nature of the molecular film.

Here, we study the CuPc/Cu(110)-(2 × 1)O interface as an example of a system where a surprisingly large change in the interfacial electronic structure is observed near a coverage of 1 monolayer. Based on a combination of scanning tunneling microscopy (STM) and angle-resolved photoemission spectroscopy (ARPES), we attribute this change to a structural transition from flat-lying, face-on CuPc molecules to a standing, edge-on molecular orientation at coverages beyond the first monolayer. This structural richness is in contrast to CuPc on Cu(110) and most organic/metal interfaces, where face-on growth over some monolayers with eventual adoption

*monti@u.arizona.edu

of the bulk organic crystal structure is the norm [16,19–21]. It is enabled by diminishing surface-molecule interactions mediated by oxygen chemisorption on Cu(110). The fact that such a structural transition is observed within a single organic/metal interfacial system permits us to interpret the large changes in the interfacial electronic structure based on simple electrostatic arguments, and provides an avenue for realizing large energy-level offsets at organic semiconductor interfaces.

II. METHODS

Copper phthalocyanine (CuPc, Sigma-Aldrich/95%) was purified by triple sublimation in a custom-built vacuum furnace (5×10^{-7} Torr). The Cu(110) crystal (Princeton Scientific) was cleaned by repeated cycles of Ar^+ sputtering (1–2 keV, $5 - 10\,\mu A/cm^2$) and annealing (850 K). Cleanliness was verified directly in STM images or by the work function [$\Phi = 4.6(1)$ eV] in ultraviolet photoemission spectroscopy (UPS). The Cu(110)-(2×1)O surface was prepared by backfilling the vacuum chamber with O_2 at low pressure ($p \sim 3.0 \times 10^{-8}$ Torr) to ensure growth of the (2×1) reconstruction. Exposures are expressed in langmuirs ($1\,L = 10^{-6}$ Torr s). Thin films of CuPc were evaporated onto room-temperature Cu(110)-(2×1)O using a home-built, water-cooled Knudsen source in a sample preparation chamber (base pressure of $<1 \times 10^{-9}$ Torr). Films were grown at a typical rate of 0.1 monolayer/min, as monitored by quartz crystal microbalance. Film thickness is reported as a fraction of a hypothetical closed monolayer (ML) of face-on molecules ($1\,ML \approx 4.44 \times 10^{13}$ molecules/cm^2) and referred to as nominal thickness.

For STM, the sample was transferred to the imaging chamber (pressure $< 10^{-11}$ Torr) immediately following sample preparation, where it remained at room temperature for 2 min before rapid quenching to 77 K and continued cooling to 5 K. All STM images were acquired at 5 K with the instrument in constant current mode. The PtIr tip was formed by electrochemical etching and further shaped with a focused ion beam. Microscope control and image processing were performed using the GXSM software package [22]. All photoemission experiments (analysis chamber pressure $<10^{-10}$ Torr) were performed at room temperature with an unpolarized Scientific Instruments UVS 200 He lamp. The energy resolution of the analyzer is approximately 70 meV as determined by Fermi-level broadening of the clean surface. Work functions were determined from spectra taken with a -5 V bias to facilitate analysis of the secondary cutoff edge. For angle-resolved experiments (ARPES), the bias was reduced to -3 V and the electron acceptance angle narrowed to $\pm 1.5^\circ$. Crystal azimuthal orientation with respect to the surface Brillouin zone was determined using low-energy electron diffraction with an estimated angle accuracy of $\pm 5^\circ$.

III. RESULTS

A. Interfacial electronic structure

Normal emission UPS data for nominal coverages of CuPc on oxidized Cu(110) are shown in Fig. 1. Prior to molecular deposition, the surface was prepared by exposure of clean Cu(110) to $\sim$24 L O_2 at 100 °C. This procedure results in a surface fully saturated with the oxygen-induced $p(2 \times 1)$ reconstruction Cu(110)-(2×1)O [23,24]. Molecular contributions to the electronic density of states (DOS) are evident with increasing nominal CuPc coverage in the spectral sequence of Fig. 1(a): Data for thicker films show very clearly the emergence of molecular features in several regions below the intense Cu(110) d bands and near the Fermi level (E_F) at binding energies ($E_F - E$) of around -1 eV. The system does not exhibit any distinct molecular feature at E_F, which would have indicated interfacial charge transfer, and is commonly encountered in strongly hybridized interfaces [17,25–27]. The accompanying work-function changes, $\Delta\Phi$, are also shown in Fig. 1(a) inset, plotted relative to pristine Cu(110)-(2×1)O [$\Phi = 4.9(1)$ eV]. The work function decreases monotonically with increasing coverage to give $\Delta\Phi = -0.54$ eV at a nominal film thickness of 4 ML. For the first monolayer of CuPc, $\Delta\Phi$ of ~ -0.32eV is comparable to titanyl phthalocyanine on bare Cu(110) [26], indicating that pushback of the surface electronic wave function is significant even for the oxidized surface.

Focusing our attention on the frontier orbital region near E_F, a molecular feature at -1.4 eV binding energy develops at low coverages [see, e.g., 0.5 ML spectrum in Fig. 1(b)]. This is the highest occupied molecular orbital (HOMO) of molecules forming the interfacial layer, i.e., in direct contact with the surface. We refer to this layer henceforth as the interface layer (IL). STM data supporting this assignment are discussed in detail below (see Fig. 3). The $HOMO_{IL}$ intensity increases with coverage until a maximum is reached between 1 and 1.5 ML, whereafter its intensity decreases. Meanwhile, an additional molecular feature at -1 eV appears at coverages near a nominally full monolayer and continues to grow with increasing coverage. Due to the behavior of this feature as a function of molecular coverage, we attribute it to the HOMO of molecules in the second layer and beyond, and label it $HOMO_{Film}$.

The relative binding energies of these two HOMOs are somewhat unusual for three salient reasons: First, the fact that the $HOMO_{IL}$ binding energy is *larger* than that of the $HOMO_{Film}$ is not consistent with simple considerations of the work-function change ($\Delta\Phi$) and interface dipole; if both features had a common electronic origin, $HOMO_{IL}$ would be expected to appear at a *lower* binding energy as the work function drops with coverage [Fig. 1(a) inset] [28,29], contrary to our findings. This indicates both that the two spectroscopic features report on electronically different CuPc species in the first few layers and that interactions beyond simple interface dipoles are significantly shaping the interfacial electronic structure. Second, when accounting for $\Delta\Phi$, the ionization energy of first-layer molecules is much greater than that of second-layer molecules (6 vs 5.4 eV), at odds with a simple polarization energy picture [30,31]. Third, the dramatic change in ionization energy occurs *abruptly* with the growth of the second layer of molecules, instead of evolving gradually as the film grows [19]. Importantly, these observations contrast with the electronic structure of CuPc on other surfaces [32–37], and instances where multiple HOMOs have been observed in phthalocyanine films [38,39]. Together and as discussed below, they point to an abrupt structural transition as the second layer forms.

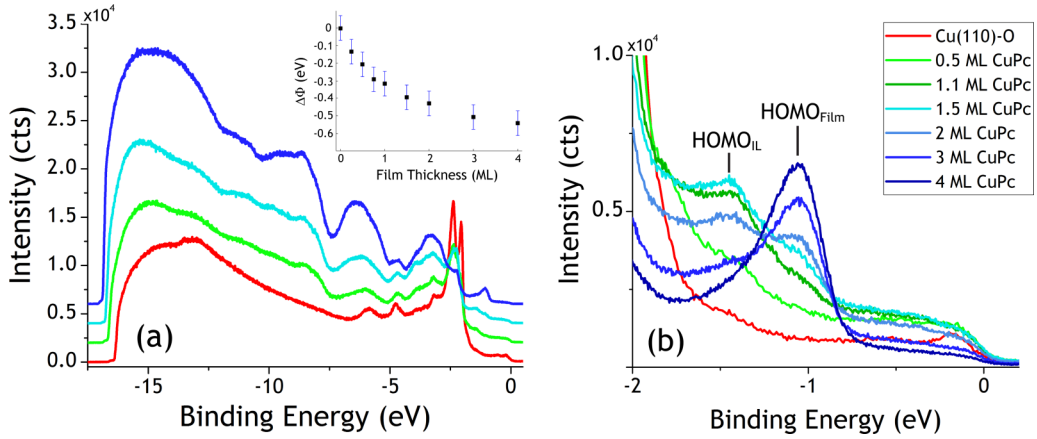

FIG. 1. (a) Normal emission UPS spectral sequence for thin-film growth of CuPc on Cu(110)-(2 × 1)O. Spectra offset for clarity. Inset: Plot of work-function change ($\Delta\Phi$) as a function of nominal film thickness. (b) Frontier orbital region evolution as a function of nominal CuPc coverage. The legend indicates nominal coverage in both panels (a) and (b).

To understand the underlying causes for the interface evolution, we consider each of these points in more detail in what follows, aided by a closer analysis of the region near E_F. Figure 2(a) shows a fit with a single Gaussian (linear background) for each of the two HOMO features in the nominally 1.5 ML film. The $HOMO_{IL}$ half width at half maximum (HWHM) [191(8) meV] is significantly wider than the $HOMO_{Film}$ HWHM [98(5) meV], an indication of some degree of coupling with the surface. The possible role of inhomogeneous broadening and substantial structural disorder in the interface layer is minor, as is evident from the STM data (see below). The $HOMO_{IL}$ and $HOMO_{Film}$ are centered at −1.469(3) and −1.096(3) eV binding energy, respectively, a difference of 373 meV. A $HOMO_{IL}$ ionization energy much greater than that of the $HOMO_{Film}$ excludes electronic polarization effects at the interface as the source of the two molecular features [30,40,41]. Additionally, not only is the *order* of HOMO energies in contradiction to expectations for polarization effects (e.g., photohole screening), but the *magnitude* of the energy difference is also significantly larger than typically observed between interface layer and the next few molecular layers, as seen, e.g., in 1–2 ML CuPc on highly oriented pyrolytic graphite (HOPG [36]), and other organic semiconductors on various surfaces [30,42–47]. The magnitude is greater even than suggested "band-bending" effects in tens of layers of CuPc on HOPG [33,48], Si(111) [32,37], Au(100) [34], and Au(110) [40]. Thus both the orbital ordering and separation show clearly that the difference between the $HOMO_{IL}$ and $HOMO_{Film}$ stems from factors beyond mere polarization effects.

Figure 2(b) shows a fit to the HOMO region of the nominally 4 ML film, again with two Gaussian functions. We do not constrain the peak positions to coincide with those at lower coverages because of changes to the polarization energy for the thicker films [49], and potential interactions between the two layers. With this model, we find that the $HOMO_{IL}$ is located at −1.321 (5) eV and the $HOMO_{Film}$ is located at −1.090(2) eV. The ionization energy of the $HOMO_{IL}$ has decreased, presumably due to photohole screening by the molecular overlayer, and the binding-energy difference between the two HOMOs has decreased to 230 meV. Surprisingly, $HOMO_{IL}$ is still clearly discernible, and rather intense even, in a film of nominally 4 ML thickness despite the limited escape depth for photoelectrons at this kinetic energy. This is a clear indication that the growth of CuPc on Cu(110)-(2 × 1)O is not simply layer-by-layer but might be attributed to island growth or instead involve a more complex structural transition.

To analyze the growth and to understand the unique behavior of the two HOMO features better, we used STM to study the structural properties of the film. Figure 3(a) shows an STM image for a nominal coverage of 0.9 ML CuPc (∼80% of terrace area covered) grown on a surface nearly saturated with the Cu(110)-(2 × 1)O reconstruction [prepared by exposure of Cu(110) at 100 °C to ∼6 L O_2; complete saturation occurs at ≈ 7 L O_2)] [24]. Individually, CuPc molecules lie with the molecular plane nearly parallel to the surface as indicated by four fully resolved and almost symmetric ligand lobes. A slight molecular tilt or distortion is evident in that some lobes appear brighter than others [Fig. 3(a) inset]. Further, molecules display a single unique adsorption configuration relative to the atomic lattice with one mirrored azimuth that results in two possible orientations, rotated by ±15° relative to [001] [black and white molecules overlaid in Fig. 3(b)]. Molecules assemble into rows of homogeneous molecular orientation directed along [001], and aggregation of parallel rows leads to the formation of monolayer CuPc islands. From the detailed view of such an island in Fig. 3(b), we observe that adjacent rows display two types of coupling depending on the spacing between rows: When the inter-row spacing is small, phenyl rings of the Pc ligand intercalate along the [001] direction; conversely, when inter-row spacing is larger, phenyl rings of adjacent molecules couple edge-to-edge along [001] [white dashed lines, Fig. 3(b)]. We infer from the staggered molecular arrangement between closely spaced rows [Fig. 3(a) inset] that intermolecular interactions include hydrogen-bond-like long-range interactions involving the aza-*N* atom and peripheral hydrogen atoms [50].

While long-range order is not present in the film, perhaps due to a symmetry mismatch between the rectangular Cu(110)-(2 × 1)O surface and the fourfold symmetry of CuPc,

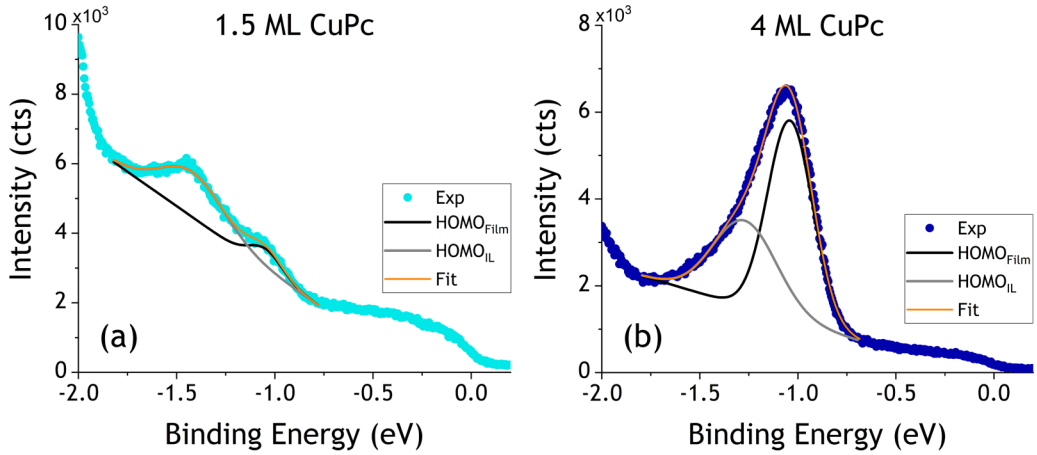

FIG. 2. (a) Fit of the $HOMO_{IL}$ and $HOMO_{Film}$ in a 1.5 ML-thick film. (b) Fit of $HOMO_{IL}$ and $HOMO_{Film}$ in a 4-ML-thick film.

the molecules order locally. We observe n-row domains of differing sizes ($n = 1, 2, 3$) coexisting within islands; 2-row domains of homogeneous molecular orientation are the most prevalent, similar to F_{16}CuPc on Ag(111) [51]. Within such domains, molecules form an almost square network with lattice parameters $b_1 = 14.1(3)$ Å, $b_2 = 14.7(4)$ Å, and $\beta = 91(2)^\circ$ with an azimuthal rotation of $\theta = 1(1)^\circ$ between b_1 and [001] [Fig. 3(a) inset] [52].

The observation of locally ordered monolayer islands contrasts with CuPc and TiOPc films on pristine Cu(110). On Cu(110), strong interactions with the surface [53] and native adatoms [20] influence both the structure and dynamics of film formation and lead to amorphous films [54]. The oxidized surface, however, weakens these interactions and captures Cu adatoms by assimilating them into the reconstructed lattice [55,56]. By removing free adatoms and mixing O character into the surface electronic wave function, oxygen chemisorption passivates the reactive Cu(110) surface, thereby allowing for local ordering of molecules in the film. The weakened surface-molecule interaction is evident also in the STM experiments, manifesting as the few noisy regions in Fig. 3(a) from adsorbate instability in the presence of the tip. Note that STM images of films with coverages exceeding nominal thicknesses of 1 ML could not be observed even at 5 K, likely due to the rather weak intermolecular interactions between different molecular layers.

Taken together and in light of the photoemission results, the STM data are rather surprising: CuPc grows in locally ordered domains, displaying a unique face-on adsorption configuration in the first layer. Even near completion of the first layer, we observe no evidence of second-layer island growth. CuPc instead forms a true interfacial wetting layer on Cu(110)-(2 × 1)O. Consequently, the origin of the unusual spectroscopic transition between $HOMO_{IL}$ and $HOMO_{Film}$ cannot be the result of island growth, but must rather lie in a profound structural transition that occurs at film thicknesses beyond 1 ML. We next investigate the nature of this film structure transition in more detail.

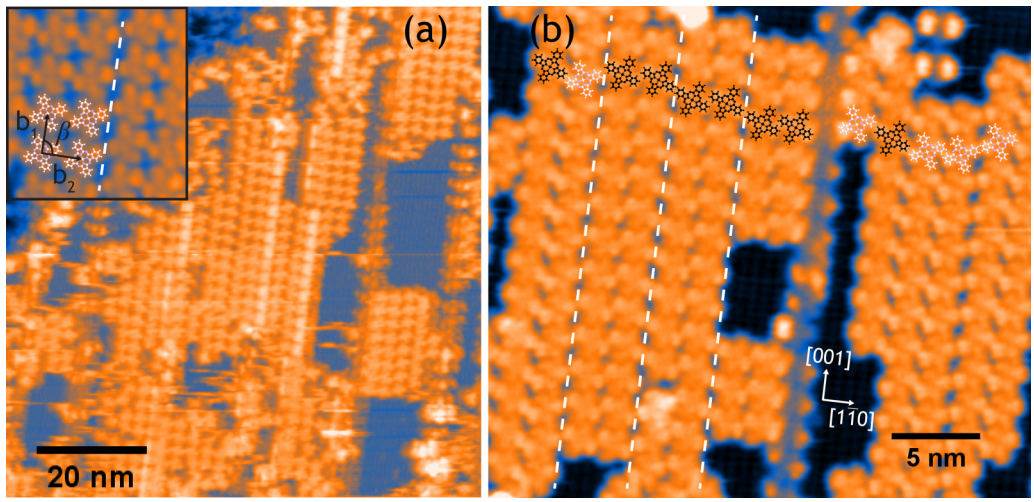

FIG. 3. (a) Overview constant current STM image of 0.9 ML CuPc grown on a nearly saturated Cu(110)-(2 × 1)O surface (sample bias $V_S = 100$ mV; tunneling current $I_T = 10$ pA). Inset: Molecular detail in islands. (b) Atomically resolved image showing structure of local molecular ordering and the underlying Cu(110)-(2 × 1)O lattice. The two orientations of CuPc molecules are indicated with light and dark molecular models, and white dashed lines demarcate larger inter-row spacing between double-row domains.

B. Structural transition

A molecular-level understanding of the film structure is essential when interpreting the interfacial electronic structure. STM alone is however not enough to understand the structure of the film beyond 1 ML, particularly given the weak interaction between molecules in the second layer and the interfacial layer even when imaging at 5 K. The STM data prove a first layer of face-on CuPc, while the direction and magnitude of the HOMO shift suggests an abrupt structural transition in the second layer. Here, we propose that a face-on to edge-on transition occurring between the interfacial layer and subsequent layers is the source of the striking electronic structure evolution in this system, similar to observations in sexithiophene derivatives on Ag(111) [18]. We emphasize that a face-on seed layer with locally ordered domains is necessary to template edge-on growth in the second layer, which can only be achieved on the oxidized surface. This is consistent with the fact that CuPc has been shown to exhibit various molecular adsorption geometries in thin films depending on the strength and type of surface-molecule interaction [37,57,58].

The existence of a structural transition is supported by the spectroscopic observations of the evolution of the HOMO ionization energy. While the ionization energy is partly determined by the far-field effect of the interface dipole, it also depends on near-field effects of the local electronic environment, i.e., the charge distribution within the molecule [59]. This has been shown clearly for the case of strongly polar intramolecular bonds [60,61], and can be expected to play an important role also when changing molecular orientation. π-conjugated molecules have significant quadrupole moments; the associated charge distribution gives rise to intrinsic electric fields across a molecule that alter the photoelectron kinetic energy and hence the observed ionization energy [18]: Photoelectrons originating from face-on molecules interact with an electron-rich π-system charge distribution (increasing ionization energy), while photoelectrons emitted from edge-on molecules sense primarily the electron-deficient hydrogen-terminated periphery of the molecule (decreasing ionization energy). Therefore, the lower ionization energy of molecules in the second layer indicates a change at the film surface in the local charge distribution toward lower electron density, consistent with edge-on CuPc molecules.

More evidence for a lying-to-standing transition comes from the very different angle dependence of the photoemission intensity for the two HOMO features. The angle dependence of the photoemission intensity reports directly on the vectorial molecular photoemission matrix element and provides thus insight into the molecular geometry relative to the surface [62]. In the case of CuPc on Cu(110)-(2×1)O, $\mathrm{HOMO_{IL}}$ and $\mathrm{HOMO_{Film}}$ have rather different angle dependence, indicating different molecular geometries. Indeed, this is seen clearly despite the presence of a strongly dispersive surface band feature in the angle-resolved data along $\bar{\Gamma}-\bar{Y}$ [Fig. 4(a)]. Although this O $2p^*$ surface band interferes somewhat with a quantitative assessment of molecular orientation particularly for $\mathrm{HOMO_{IL}}$, we are still able to compare the polar angle-dependent photoemission intensity with simulations for both face- and edge-on adsorption geometries. To this end we make use of the plane-wave final state formalism developed for photoemission tomography [63,64]. In this framework, the photoemission intensity at a certain energy is proportional to the Fourier transform of the initial state wave function. We calculate this for the CuPc HOMO in both a face-on and a fully edge-on geometry, and obtain polar- and azimuthal angle-dependent photoemission intensities as shown in the maps in Figs. 4(b) and 4(d). For simplicity's sake, we ignore the contributions of disorder and mirror domains (see Fig. 3) and calculate lineouts along the appropriate directions given molecular orientation on the surface with respect to the underlying Cu(110)-(2×1)O surface. For the face-on $\mathrm{HOMO_{IL}}$ and the experimental photoemission intensity in Fig. 4(a) obtained along $\bar{\Gamma}-\bar{Y}$, the relevant lineout is taken along a ray rotated by 15° in order to represent the molecular orientation with respect to the surface. A comparison of the calculated intensity with the experimental values is shown in Fig. 4(c). In light of the influence of the $2p^*$ surface band, both experiment and simulation exhibit reasonable agreement, with maxima near 1 $\mathrm{Å}^{-1}$ and a shoulder near 0.4 $\mathrm{Å}^{-1}$. Overall this is not surprising, since a face-on orientation for an interfacial layer is expected on this and other metallic surfaces. More interestingly, the simulation of the edge-on geometry is fully consistent with the experimental polar angle-dependent photoemission intensity of $\mathrm{HOMO_{Film}}$ [Fig. 4(e)]. For this simulation, we assume a pure rotation to the edge-on orientation, with the vector normal to the molecular plane directed 15° relative to $\bar{\Gamma}-\bar{Y}$. We note however that the azimuthal orientation of the molecules in the second layer and beyond is unknown from our STM studies, as discussed earlier.

From the comparison of experimental and simulated data, we find that the angle dependence of photoemission intensity for the $\mathrm{HOMO_{IL}}$ and $\mathrm{HOMO_{Film}}$ are conclusively different, and can be explained by different molecular geometries in the first and second layer. Along $\bar{\Gamma}-\bar{X}$ (not shown), interference from a strong Cu(110) sp-band direct transition [65] completely obscures the HOMO features, prohibiting further assessment of the specific azimuthal orientation of edge-on molecules in the second layer. Nevertheless, both angle dependence and relative ionization energies suggest that molecules in the second layer orient differently in general, and with the molecular plane more normal to the surface.

The proposed structural transition affects our interpretation of electronic structure measurements when considering the reported film thickness: with the molecular plane preferentially oriented toward the surface normal, the molecular packing density changes dramatically in the second layer. This means that reported (nominal) coverages above 1 ML, based on a hypothetical ML of face-on molecules, are in reality much lower: Estimating from crystal structures the separation between edge-on molecules to be ∼3.5 Å [66,67], approximately four times the number of molecules are required to form a full layer of edge-on molecules. Our nominal 4 ML coverage in Fig. 1, established on the assumption of face-on layer-by-layer growth, corresponds thus rather to actual 1.75 ML, consisting of a full first layer of face-on molecules and an incomplete second layer of edge-on molecules. This readily explains the originally puzzling observation of a $\mathrm{HOMO_{IL}}$ at nominal

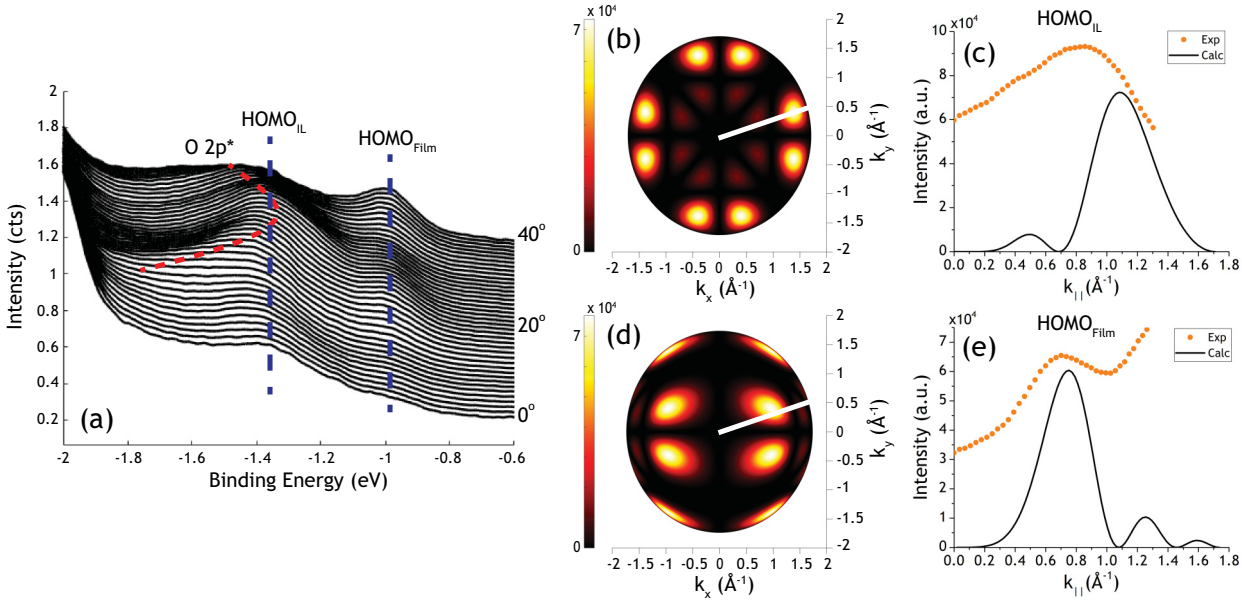

FIG. 4. (a) Photoemission intensity obtained along $\bar{\Gamma} - \bar{Y}$ for both $HOMO_{IL}$ and $HOMO_{Film}$. (b), (d) Azimuth and polar angle-dependent photoemission intensity calculated in the plane-wave final state approximation for face-on and edge-on adsorption geometries of CuPc, at binding energies of $HOMO_{IL}$ and $HOMO_{Film}$, respectively. The solid white lines indicate the $\bar{\Gamma} - \bar{Y}$ direction given a molecular rotation by 15° with respect to [001]. (c), (e) Comparison of experimental and calculated photoemission intensities.

coverages of 4 ML of face-on molecules, a film thickness that would be expected to exceed the photoelectron escape depth at these kinetic energies. Instead, partial closure only of the second, edge-on layer (true coverage of 1.75 ML) leaves 25% of the IL CuPc exposed and explains the observable $HOMO_{IL}$ at this coverage. Moreover, this is also consistent with the facts that $\Delta\Phi$ (i) is not yet converged at a nominal coverage of 4 ML (actual 1.75 ML) and (ii) increases smoothly rather than abruptly owing to the gradual growth of the second ML. Note however that the difference in work function, $\Delta\Delta\Phi$, for true coverages of 1 and 1.75 ML, is −0.225 eV, quite large and consistent with a molecular reorientation in the second layer.

C. Surface-molecule coupling

It is important to test our explanation of the interfacial electronic structure against alternative explanations. A likely alternate hypothesis for the abrupt change in HOMO ionization energy might be strong coupling of the first molecular layer to the surface, which would give rise to new and different molecular features at the interface. Fortunately, the electronic structure of the oxidized surface contains ideal markers for assessing the nature of electronic coupling between the surface and the molecular film. Because oxygen atoms exist only in the surface reconstruction, electrons in bands with oxygen character are localized at the crystal surface [68], and thus extremely sensitive to molecular adsorption, similar to Shockley surface states on coinage metal (111) surfaces [69,70]. Along $\bar{\Gamma} - \bar{Y}$, these bands disperse well beyond the bandwidth of the molecular DOS at similar energies [23,71–74], allowing us to test molecular adsorption effects on band dispersion as an indicator of the extent of interfacial hybridization in the first molecular layer. Figure 5 gives the experimental band diagram for Cu(110)-(2 × 1)O along $\bar{\Gamma} - \bar{Y}$, with bands derived from oxygen $2p$ orbitals indicated by white dashed lines. We note that neither the Cu(110) surface state nor the antibonding oxygen $2p_y$ band are observed: The former shifts above E_F on the reconstructed surface, and the latter mixes strongly with bulk Cu states and cannot be distinguished any longer [68].

Figure 6 shows how thin-film growth of the first ML modifies these bands. From the 0.25 ML CuPc data [Fig. 6(a)], we see that the presence of molecules barely affects the dispersion of the surface bands. Because CuPc forms ordered islands, the majority of the surface sampled by photoemission

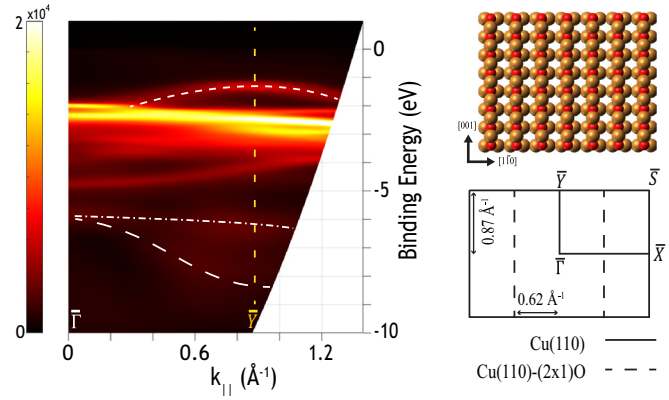

FIG. 5. Background-subtracted ARPES data for pristine Cu(110)-(2 × 1)O along $\bar{\Gamma} - \bar{Y}$. Bands with oxygen $2p$ character are indicated by white dashed lines: short dashed - antibonding $2p_x$ and $2p_z$, dashed dot - bonding $2p_x$ and $2p_z$, long dashed - bonding $2p_y$. Intense features between −2 and −5 eV are Cu(110) d bands. Also shown is a cartoon of the Cu(110)-(2 × 1)O lattice and the respective Brillouin zone.

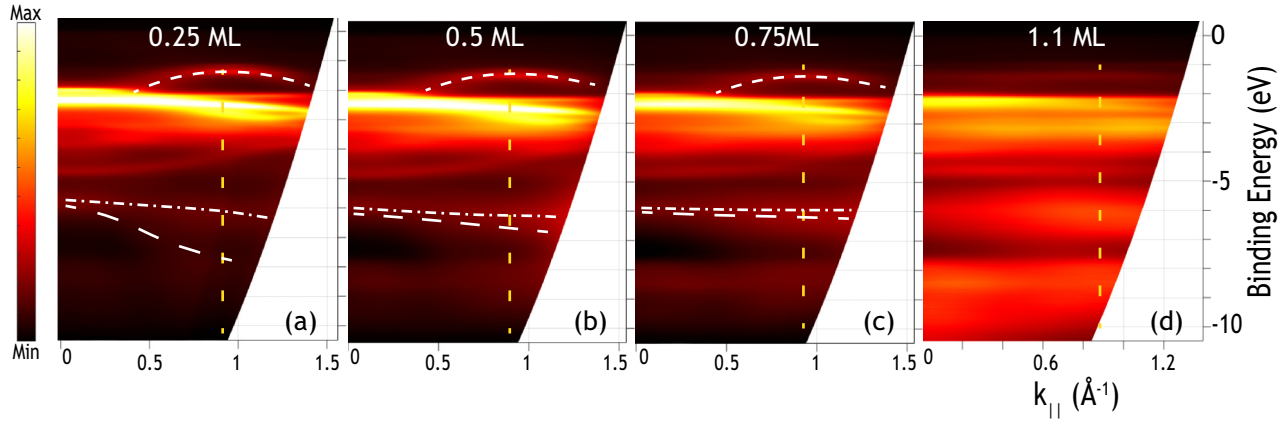

FIG. 6. The effect of CuPc growth on the band structure of Cu(110)-(2 × 1)O. Bands with oxygen $2p$ character are indicated as in Fig. 5: short dashed - antibonding $2p_x$ and $2p_z$, dashed dot - bonding $2p_x$ and $2p_z$, long dashed - bonding $2p_y$. The $\bar{Y}$ point of the surface Brillouin zone is indicated with a yellow dashed line. (a) 0.25 ML CuPc. (b) 0.5 ML CuPc. (c) 0.75 ML CuPc. (d) 1.1 ML CuPc.

is still pristine Cu(110)-(2 × 1)O. At 0.5 ML CuPc, however, photoemission from the molecular film is significant enough to show a localization of the oxygen $2p_y$-derived band [long dashed line in Fig. 6(b)]. This may be caused by photoelectron scattering at the molecular layer, which would obscure the electron momentum during the photoemission process [75]. Remarkably however, neither the bonding nor the antibonding O $2p_x$ and $2p_z$ bands undergo large changes to their dispersion. It is thus likely that the observed decrease in dispersion in the O $2p_y$ band is in fact due to hybridization with a nondispersive molecular feature at ~ -6 to -7 eV binding energy [see also Fig. 1(a)]. We propose that this selective hybridization is a result of the near-degeneracy between the O $2p_y$ band and a number of lower-lying molecular orbitals, together with a symmetry match only with the O $2p_y$ band toward $\bar{Y}$.

By 0.75 ML, the oxygen $2p_y$ band is completely localized and indistinguishable from the broad molecular feature, while the antibonding oxygen $2p_x$- and $2p_z$-derived bands are still clearly visible [Fig. 6(c)] without exhibiting major changes to their dispersion. The angle-resolved data for 1.1 ML CuPc overwhelmingly project the nondispersive molecular DOS [Fig. 6(d)], but as can be seen more clearly in Fig. 4, the antibonding oxygen $2p_x$- and $2p_z$-derived bands can still be observed upon close inspection, and they still disperse significantly. In contrast and at all coverages, the HOMO_{IL} remains entirely localized. Together with weak direct intermolecular coupling, the low degree of surface-molecule coupling does not enhance intermolecular coupling sufficiently to delocalize molecular features, in contrast to observations in ordered and strongly coupled interfaces of pentacene on Cu(110) [76].

The conclusion from the angle-resolved data must therefore be that while some hybridization is occurring between the surface and the molecules, especially in lower-lying orbitals, electronic coupling of CuPc frontier orbitals to the surface and creation of new interfacial states is quite minimal. Furthermore, the survival and dispersion of the antibonding surface bands also demonstrates that significant distortion of the surface lattice does not occur upon adsorption of the molecule. These observations, together with the mobility of first-layer molecules even at 5 K [evident from STM image noise in Fig. 3(a)], allow us to conclude that the two different HOMO levels are *not* due to strong coupling of the molecules in the first layer followed by layer decoupling, and are instead the result of a structural transition in the film.

D. Summary of interfacial energetics

To summarize our findings, an energy-level diagram is presented in Fig. 7. We calculate ionization energies only from mostly complete layers to avoid complications due to local vacuum level variations in the presence of distributed island growth. Molecules in the first full layer of CuPc on Cu(110)-(2 × 1)O adsorb face-on to the surface with the HOMO_{IL} centered at ~ -1.5 eV below E_F [Fig. 7(a)] to give an ionization energy of 6.05(7) eV, which is in line with reports of CuPc on other surfaces [77]. Initial growth of the second layer shows a $\text{HOMO}_{\text{Film}}$ binding energy ∼370 meV lower than that of the HOMO_{IL} [Fig. 7(b)]. The ionization energy for a molecule in a nearly full second layer is 5.43(7) eV [Figs. 7(a) and 7(c)], a drop of over 0.6 eV from the interfacial layer. Such a dramatic change in ionization energy, which includes contributions from the work-function change $\Delta\Delta\Phi$ of -0.225 eV between films, is best understood by an abrupt transition to edge-on CuPc growth in the second layer. The magnitude of the change in ionization energy is comparable to that for the case of reorientation of sexithiophenes on Ag(111) [18]. The observation of such electronic and structural effects, supported by both ARPES and STM, enables us to offer a straightforward interpretation of the influence of different thin-film phases on the interfacial electronic structure for the case of CuPc on Cu(110)-(2 × 1)O. More generally, it indicates clearly that the thin-film structure can be of overriding importance in considerations of energy-level alignment at organic/metal interfaces. Furthermore, we have demonstrated that surface modification by oxygen chemisorption is critical for ordered first-layer growth, suppressing cooperative nanoribbon formation on the reactive Cu(110) surface. The interface layer templates edge-on second layer growth and ultimately leads to the striking changes in electronic structure observed in the bilayer film.

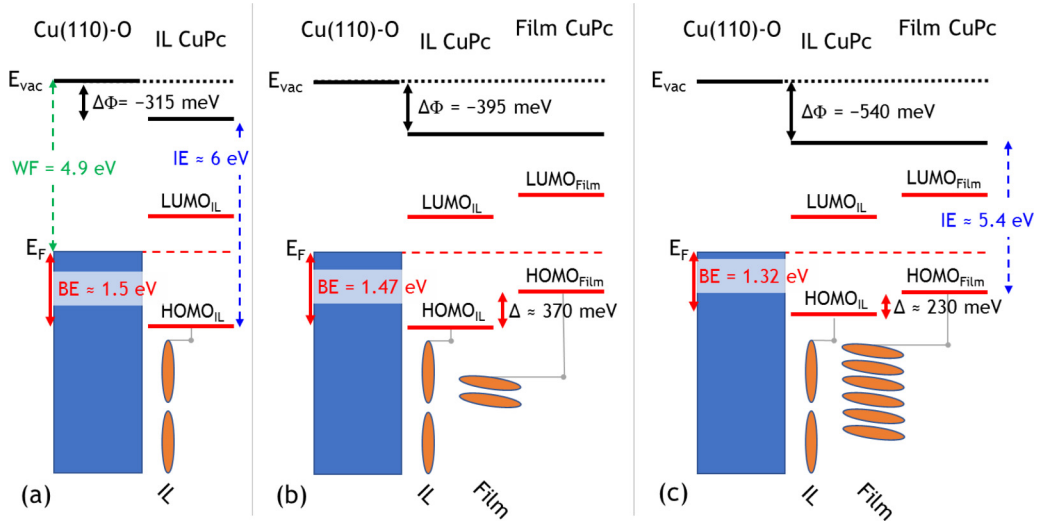

FIG. 7. Energy-level diagram for the growth of CuPc on Cu(110)-(2 × 1)O. (a) 1 ML CuPc: Molecules adsorb face-on to the surface in the interface (first) layer (IL). (b) ∼1.25 ML CuPc: Upon saturation of the IL, the next layer of molecules grows in an edge-on orientation. Due to the changing packing density, these coverages do not correspond to those in previous figures. (c) ∼1.75 ML CuPc: The nearly full second layer of edge-on molecules.

IV. CONCLUSIONS

In conclusion, we observe a unique evolution of interfacial electronic structure for CuPc films on Cu(110)-(2 × 1)O, and show that this behavior is the result of an abrupt transition in film structure between the first and second layers. The presence of two different coverage-dependent thin-film phases for a single organic/metal interface enables us to interpret changes to the interfacial electronic structure directly based on simple electrostatic arguments. Specifically, we show that oxygen chemisorption on the Cu(110) surface enables growth of an interface layer of locally ordered, face-on molecules which template an edge-on orientation for CuPc in the subsequent layer. The anisotropic charge distribution in CuPc drastically decreases the HOMO ionization energy for edge-on molecules, and the effect of this structural transition on interfacial energetics is a 600-meV ionization energy drop between the interfacial layer and subsequent layers. The results of our findings have important implications for organic electronics [18]: Large energy-level offsets can be realized between two adjacent thin-film layers and with only one molecular species, two properties that are important for the miniaturization and functionality of electronic devices. In summary, we have shown that influencing interfacial interactions through a precisely controlled modification of the surface atomic structure is a simple and effective way to tailor the structural and electronic properties of organic semiconductor interfaces.

ACKNOWLEDGMENTS

This research was supported by the National Science Foundation under Grants No. CHE-1213243 and No. CHE-1565497 as well as the Arizona TRIF imaging fellowship. This research used resources of the Center for Functional Nanomaterials, which is a US Department of Energy Office of Science Facility, at Brookhaven National Laboratory under Contract No. DE-SC0012704. We gratefully acknowledge fruitful discussions and help from Felix Otto and Torsten Fritz (Friedrich Schiller Universität Jena, Germany).

[1] K. A. Mazzio and C. K. Luscombe, Chem. Soc. Rev. **44**, 78 (2015).
[2] P. M. Beaujuge and J. M. J. Fréchet, J. Am. Chem. Soc. **133**, 20009 (2011).
[3] C. Liao and F. Yan, Polym. Rev. **53**, 352 (2013).
[4] A. Mishra and P. Bäuerle, Angew. Chem., Int. Ed. Engl. **51**, 2020 (2012).
[5] D. A. Egger, Z.-F. Liu, J. B. Neaton, and L. Kronik, Nano Lett. **15**, 2448 (2015).
[6] H. Vázquez, Y. J. Dappe, J. Ortega, and F. Flores, J. Chem. Phys. **126**, 144703 (2007).
[7] M. Oehzelt, N. Koch, and G. Heimel, Nat. Commun. **5**, 4174 (2014).
[8] A. Natan, L. Kronik, H. Haick, and R. T. Tung, Adv. Mater. **19**, 4103 (2007).
[9] W. Liu, J. Carrasco, B. Santra, A. Michaelides, M. Scheffler, and A. Tkatchenko, Phys. Rev. B **86**, 245405 (2012).
[10] O. L. A. Monti, J. Phys. Chem. Lett. **3**, 2342 (2012).
[11] A. Schöll, L. Kilian, Y. Zou, J. Ziroff, S. Hame, F. Reinert, E. Umbach, and R. H. Fink, Science **329**, 303 (2010).
[12] M. Wießner, D. Hauschild, A. Schöll, F. Reinert, V. Feyer, K. Winkler, and B. Krömker, Phys. Rev. B **86**, 045417 (2012).
[13] L. Kilian, A. Hauschild, R. Temirov, S. Soubatch, A. Schöll, A. Bendounan, F. Reinert, T. L. Lee, F. S. Tautz, M. Sokolowski, and E. Umbach, Phys. Rev. Lett. **100**, 136103 (2008).

[14] O. T. Hofmann, H. Glowatzki, C. Bürker, G. M. Rangger, B. Bröker, J. Niederhausen, T. Hosokai, I. Salzmann, R.-P. Blum, R. Rieger, A. Vollmer, P. Rajput, A. Gerlach, K. Müllen, F. Schreiber, E. Zojer, N. Koch, and S. Duhm, J. Phys. Chem. C **121**, 24657 (2017).

[15] M. Willenbockel, D. Lüftner, B. Stadtmüller, G. Koller, C. Kumpf, S. Soubatch, P. Puschnig, M. G. Ramsey, and F. S. Tautz, Phys. Chem. Chem. Phys. **17**, 1530 (2015).

[16] K. Xiao, W. Deng, J. K. Keum, M. Yoon, I. V Vlassiouk, W. Kendal, A. Li, I. I. Kravchenko, G. Gu, E. A. Payzant, G. Sumpter, S. C. Smith, J. F. Browning, D. B. Geohegan, K. W. Clark, E. A. Payzant, B. G. Sumpter, S. C. Smith, and F. James, J. Am. Chem. Soc. **135**, 3680 (2013).

[17] M. Hollerer, D. Lüftner, P. Hurdax, T. Ules, S. Soubatch, F. S. Tautz, G. Koller, P. Puschnig, M. Sterrer, and M. G. Ramsey, ACS Nano **11**, 6252 (2017).

[18] S. Duhm, G. Heimel, I. Salzmann, H. Glowatzki, R. L. Johnson, A. Vollmer, J. P. Rabe, and N. Koch, Nat. Mater. **7**, 326 (2008).

[19] M. Takada and H. Tada, Chem. Phys. Lett. **392**, 265 (2004).

[20] B. Maughan, P. Zahl, P. Sutter, and O. L. A. Monti, J. Phys. Chem. C **119**, 27416 (2015).

[21] I. Kröger, B. Stadtmüller, and C. Kumpf, New J. Phys. **18**, 113022 (2016).

[22] P. Zahl, T. Wagner, R. Möller, and A. Klust, J. Vac. Sci. Technol. B **28**, C4E39 (2010).

[23] R. A. DiDio, D. M. Zehner, and E. W. Plummer, J. Vac. Sci. Technol. A **2**, 852 (1984).

[24] J. F. Wendelken, Surf. Sci. **108**, 605 (1981).

[25] Y. Zou, L. Kilian, A. Schöll, T. Schmidt, R. Fink, and E. Umbach, Surf. Sci. **600**, 1240 (2006).

[26] B. Maughan, P. Zahl, P. Sutter, and O. L. A. Monti, Phys. Rev. B **96**, 235133 (2017).

[27] N. Ilyas and O. L. A. Monti, Phys. Rev. B **90**, 125435 (2014).

[28] N. Koch, A. Kahn, J. Ghijsen, J. J. Pireaux, J. Schwartz, R. L. Johnson, and A. Elschner, Appl. Phys. Lett. **82**, 70 (2003).

[29] G. Heimel, L. Romaner, E. Zojer, and J.-L. Bredas, Acc. Chem. Res. **41**, 721 (2008).

[30] E. V. Tsiper, Z. G. Soos, W. Gao, and A. Kahn, Chem. Phys. Lett. **360**, 47 (2002).

[31] H. Fukagawa, H. Yamane, T. Kataoka, S. Kera, M. Nakamura, K. Kudo, and N. Ueno, Phys. Rev. B **73**, 245310 (2006).

[32] M. Gorgoi and D. R. T. Zahn, Org. Electron. **6**, 168 (2005).

[33] T. Sugiyama, T. Sasaki, S. Kera, N. Ueno, and T. Munakata, Appl. Phys. Lett. **89**, 202116 (2006).

[34] H. Peisert, M. Knupfer, T. Schwieger, J. M. Auerhammer, M. S. Golden, and J. Fink, J. Appl. Phys. **91**, 4872 (2002).

[35] S. Sinha and M. Mukherjee, Appl. Surf. Sci. **353**, 540 (2015).

[36] S. Kera, Y. Yabuuchi, H. Yamane, H. Setoyama, K. K. Okudaira, A. Kahn, and N. Ueno, Phys. Rev. B **70**, 085304 (2004).

[37] S. Menzli, A. Laribi, H. Mrezguia, I. Arbi, A. Akremi, C. Chefi, F. Chérioux, and F. Palmino, Surf. Sci. **654**, 39 (2016).

[38] M. Toader, P. Shukrynau, M. Knupfer, D. R. T. Zahn, and M. Hietschold, Langmuir **28**, 13325 (2012).

[39] F. Petraki, H. Peisert, U. Aygül, F. Latteyer, J. Uihlein, A. Vollmer, and T. Chassé, J. Phys. Chem. C **116**, 11110 (2012).

[40] F. Evangelista, A. Ruocco, R. Gotter, A. Cossaro, L. Floreano, A. Morgante, F. Crispoldi, M. G. Betti, and C. Mariani, J. Chem. Phys. **131**, 174710 (2009).

[41] W. R. Salaneck, Phys. Rev. Lett. **40**, 60 (1978).

[42] A. Terentjevs, M. P. Steele, M. L. Blumenfeld, N. Ilyas, L. L. Kelly, E. Fabiano, O. L. A. Monti, and F. Della Sala, J. Phys. Chem. C **115**, 21128 (2011).

[43] N. Ilyas, L. L. Kelly, and O. L. A. Monti, Mol. Phys. **111**, 2175 (2013).

[44] M. P. Steele, M. L. Blumenfeld, and O. L. A. Monti, J. Chem. Phys. **133**, 124701 (2010).

[45] M. L. Blumenfeld, M. P. Steele, N. Ilyas, and O. L. A. Monti, Surf. Sci. **604**, 1649 (2010).

[46] L. Giovanelli, P. Amsalem, T. Angot, L. Petaccia, S. Gorovikov, L. Porte, A. Goldoni, and J. M. Themlin, Phys. Rev. B **82**, 125431 (2010).

[47] I. G. Hill, A. J. Mäkinen, and Z. H. Kafafi, J. Appl. Phys. **88**, 889 (2000).

[48] Y. Tao, H. Mao, and P. He, J. Appl. Phys. **117**, 013701 (2015).

[49] S. M. Ryno, C. Risko, and J. L. Bredas, ACS Appl. Mater. Interfaces **8**, 14053 (2016).

[50] C. Chiang, C. Xu, Z. Han, and W. Ho, Science **344**, 885 (2014).

[51] H. Huang, W. Chen, and A. T. S. Wee, J. Phys. Chem. C **112**, 14913 (2008).

[52] D. E. Hooks, T. Fritz, and M. D. Ward, Adv. Mater. **13**, 227 (2001).

[53] B. Maughan, P. Zahl, P. Sutter, and O. L. A. Monti, J. Phys. Chem. Lett. **8**, 1837 (2017).

[54] M. Abadía, R. González-Moreno, A. Sarasola, G. Otero-Irurueta, A. Verdini, L. Floreano, A. Garcia-Lekue, and C. Rogero, J. Phys. Chem. C **118**, 29704 (2014).

[55] F. Jensen, F. Besenbacher, E. Laegsgaard, and I. Stensgaard, Phys. Rev. B **41**, 10233 (1990).

[56] F. Besenbacher and J. K. Nørskov, Prog. Surf. Sci. **44**, 5 (1993).

[57] C. Wang, X. Liu, C. Wang, X. Xu, Y. Li, F. Xie, and Y. Gao, Appl. Phys. Lett. **106**, 121603 (2015).

[58] I. Biswas, H. Peisert, M. Nagel, M. B. Casu, S. Schuppler, P. Nagel, E. Pellegrin, and T. Chassé, J. Chem. Phys. **126**, 174704 (2007).

[59] M. L. Blumenfeld, M. P. Steele, and O. L. A. Monti, J. Phys. Chem. Lett. **1**, 145 (2010).

[60] I. Salzmann, S. Duhm, G. Heimel, M. Oehzelt, R. Kniprath, R. L. Johnson, J. P. Rabe, and N. Koch, J. Am. Chem. Soc. **130**, 12870 (2008).

[61] S. Duhm, I. Salzmann, G. Heimel, M. Oehzelt, A. Haase, R. L. Johnson, J. P. Rabe, and N. Koch, Appl. Phys. Lett. **94**, 033304 (2009).

[62] S. Hasegawa, S. Tanaka, Y. Yamashita, H. Inokuchi, H. Fujimoto, K. Kamiya, K. Seki, and N. Ueno, Phys. Rev. B **48**, 2596 (1993).

[63] K. Schönauer, S. Weiss, V. Feyer, D. Lüftner, B. Stadtmüller, D. Schwarz, T. Sueyoshi, C. Kumpf, P. Puschnig, M. G. Ramsey, F. S. Tautz, and S. Soubatch, Phys. Rev. B **94**, 205144 (2016).

[64] P. Puschnig, S. Berkebile, A. J. Fleming, G. Koller, K. Emtsev, T. Seyller, J. D. Riley, C. Ambrosch-Draxl, F. P. Netzer, and M. G. Ramsey, Science **326**, 702 (2009).

[65] K. Berge and A. Goldmann, Surf. Sci. **540**, 97 (2003).

[66] R. D. Gould, Coord. Chem. Rev. **156**, 237 (1996).

[67] X. Chen, Y. S. Fu, S. H. Ji, T. Zhang, P. Cheng, X. C. Ma, X. L. Zou, W. H. Duan, J. F. Jia, and Q. K. Xue, Phys. Rev. Lett. **101**, 197208 (2008).

[68] P. Cabrera-Sanfelix, C. Lin, A. Arnau, and D. Sánchez-Portal, J. Phys.: Condens. Matter **25**, 135003 (2013).

[69] C. H. Schwalb, S. Sachs, M. Marks, A. Schöll, F. Reinert, E. Umbach, and U. Höfer, Phys. Rev. Lett. **101**, 146801 (2008).
[70] B. W. Caplins, D. E. Suich, A. J. Shearer, and C. B. Harris, J. Phys. Chem. Lett. **5**, 1679 (2014).
[71] R. Courths, S. Hüfner, P. Kemkes, and G. Wiesen, Surf. Sci. **376**, 43 (1997).
[72] F. Pforte, A. Gerlach, A. Goldmann, R. Matzdorf, J. Braun, and A. Postnikov, Phys. Rev. B **63**, 165405 (2001).
[73] R. Ozawa, A. Yamane, K. Morikawa, M. Ohwada, K. Suzuki, and H. Fukutani, Surf. Sci. **346**, 237 (1996).
[74] R. Matzdorf and A. Goldmann, Surf. Sci. **413**, 61 (1998).
[75] L. Giovanelli, F. C. Bocquet, P. Amsalem, H. L. Lee, M. Abel, S. Clair, M. Koudia, T. Faury, L. Petaccia, D. Topwal, E. Salomon, T. Angot, A. A. Cafolla, N. Koch, L. Porte, A. Goldoni, and J. M. Themlin, Phys. Rev. B **87**, 035413 (2013).
[76] H. Yamane, D. Yoshimura, E. Kawabe, R. Sumii, K. Kanai, Y. Ouchi, N. Ueno, and K. Seki, Phys. Rev. B **76**, 165436 (2007).
[77] T. S. Ellis, K. T. Park, S. L. Hulbert, M. D. Ulrich, and J. E. Rowe, J. Appl. Phys. **95**, 982 (2004).